

Anisotropy of flux trapping in $\text{Pb}_2\text{Sr}_2\text{Y}_{0.3}\text{Ca}_{0.7}\text{Cu}_3\text{O}_8$ single crystals

S. Koleśnik, T. Skośkiewicz, and J. Igalson

Institute of Physics, Polish Academy of Sciences, Al. Lotników 32/46, 02-668 Warsaw, Poland

Z. Korczak

Institute of Physics, Maria Curie-Skłodowska University, Pl. M. Curie-Skłodowskiej 1, 20-031 Lublin, Poland

(Received 21 June 1991; revised manuscript received 29 January 1992)

The angular dependence of magnetization of single crystals of $\text{Pb}_2\text{Sr}_2\text{Y}_{0.3}\text{Ca}_{0.7}\text{Cu}_3\text{O}_8$ has been studied for various cooling procedures. A series of samples with different demagnetizing factors has been prepared. We succeeded in separating the material anisotropy from the sample shape anisotropy in the magnetization measurements. It is shown that the “field-cooled” magnetization is independent of the shape of the sample and reflects the anisotropy of the magnetic flux trapping. We observe that the vortices are most trapped in the direction parallel to the Cu-O planes. Our results are consistent with the anisotropy of the irreversibility line observed in high- T_c superconductors.

The layered crystal structure of high- T_c superconductors (HTSC), produces anisotropy of many of their physical properties such as electrical resistivity, critical magnetic fields, and magnetization. A phenomenological effective mass tensor approach predicts the “easy” direction for the magnetic vortices parallel to the c axis.^{1,2} However, weak coupling of layers allows formation of Josephson vortices along a - b planes.³ The vortices located between the layers could be strongly pinned due to the layered structure.⁴ Felner *et al.*⁵ and Tuominen *et al.*⁶ reported experimental evidence for the existence of the vortex “easy” direction parallel to the c axis, and preferential trapping of the vortices in this direction. Earlier, we have pointed out the relevance of demagnetizing effects in the interpretation of the remanent magnetization measurements.⁷ The angular dependence of the magnetization could be substantially affected by the shape of the crystal.

The main purpose of this paper is to show the material anisotropy of the flux trapping and pinning in a single crystal of HTSC. In our experiment we used a $\text{Pb}_2\text{Sr}_2\text{Y}_{0.3}\text{Ca}_{0.7}\text{Cu}_3\text{O}_8$ single crystal. Crystals of this compound grow relatively well in the c direction, giving samples up to 0.3 mm thick in the c direction. We were able to prepare a sample with almost equal dimensions parallel to the c axis and parallel to the a - b planes. Therefore we could perform magnetization measurements on the sample with equal demagnetizing factors in these two directions.

The magnetically measured onset of the superconducting transition of our crystal is 78 K. Preparation and basic characteristics of this material have been described elsewhere.⁸ Magnetization measurements were initially performed on a single crystal of dimensions $1.06 \times 0.95 \times 0.28$ mm³, denoted as No. 1 in Table I. Then the crystal was cut into two parts by means of a wire saw, and the measurements were repeated. The dimensions of these two samples (Nos. 2 and 3) are also given in Table I.

We used a superconducting quantum interference de-

vice (SQUID) magnetometer for magnetization measurements. The external magnetic field was applied along the magnetometer axis. The magnetometer was equipped with a rotary sample holder, whose axis of rotation was perpendicular to the magnetometer axis and parallel to the a - b planes of the crystal. The projections of the zero-field-cooled magnetization (M_{ZFC}), field-cooled magnetization (M_{FC}), and remanent magnetization (M_{REM}) on the direction of the magnetometer axis were measured for each of the crystals. In the case of the zero-field-cooling (ZFC) procedure, the sample was cooled down below T_c in an ambient magnetic field (approximately 50 mOe). The magnetic field $H = 10$ Oe (well below H_{c1}) was switched on at $T = 4.2$ K. The crystal was then rotated in the magnetic field \mathbf{H} and the angular dependence of M_{ZFC} was measured. The rotation angle Θ is the angle between the magnetometer axis and the c axis of the crystal (Fig. 1). In the case of the field-cooling (FC) procedure, the sample was cooled in the magnetic field of 10 Oe at a certain “cooling angle” Φ between \mathbf{H} and the c axis of the crystal. M_{FC} was measured at $T = 4.2$ K. Then the field was switched off and the initial remanent magnetization M_{REM}^i was measured. The angular dependencies of $M_{FC}(\Theta)$ and $M_{REM}(\Theta)$ were measured during the rotation of the crystal.

The results of the measurements of M_{ZFC} , M_{FC} , and

TABLE I. Dimensions and demagnetizing factors of $\text{Pb}_2\text{Sr}_2\text{Y}_{0.3}\text{Ca}_{0.7}\text{Cu}_3\text{O}_8$ single crystals. Demagnetizing factors are calculated from the dimensions of the crystals using an approximation of the shape of the sample as an ellipsoid.

Crystal	Dimensions (mm)			Demagnetizing factors	
	In a - b plane		Along c axis	M	N
No. 1	1.06	0.95	0.28	0.17	0.68
No. 2	1.06	0.62	0.28	0.26	0.62
No. 3	1.06	0.25	0.27	0.48	0.45

M_{REM}^i are presented in Figs. 2(a), 2(b), and 2(c) for crystals No. 1, No. 2, and No. 3, respectively. The horizontal axis of the figures is the rotation angle Θ for M_{ZFC} , and the cooling angle Φ for M_{FC} and M_{REM}^i measurements.

In our experimental data the formula $M_{\text{REM}}^i = M_{\text{FC}} - M_{\text{ZFC}}$, predicted by the flux-pinning theory, is fulfilled with a good accuracy for all angles.

The ZFC magnetization of the superconductor below H_{c1} is the result of the complete exclusion of the flux from the sample. The angular dependence of M_{ZFC} reflects the variation of the demagnetizing factor of the sample. We approximate the shape of our crystal as an ellipsoid with principal axes equal to the dimensions of the crystal. The internal field (\mathbf{H}_I) is related to the applied field (\mathbf{H}_A) as follows:

$$H_{Ij} = H_{Aj}(1 + 4\pi D_j \chi)^{-1}, \quad (1)$$

$j = x, y, z$ and the z direction is parallel to the c axis of the sample. D_j are demagnetizing factors for the field applied parallel to the principal axes⁹ usually labeled L, M, N for axes x, y, z , respectively. The magnetic field is applied in the y - z plane (Fig. 1) and the sample is rotated around the x axis. The absolute value of the internal field as a function of the rotation angle Θ follows the formula

$$H_I(\Theta) = H_A[(1-M)^{-2} \sin^2 \Theta + (1-N)^{-2} \cos^2 \Theta]^{1/2}. \quad (2)$$

Our SQUID magnetometer measures the projection of the magnetization on the magnetometer axis

$$M_{\text{ZFC}} = \chi H_I \cos(\Theta - \Psi) \quad (3)$$

(Ψ is the angle between the internal field H_I and the z axis; see Fig. 1). Taking into account that

$$\tan \Psi = H_{Iy}/H_{Iz} = (1-N)(1-M)^{-1} \tan \Theta, \quad (4)$$

Eq. (2) can be transformed to

$$M_{\text{ZFC}} = \chi H_A [(1-M)^{-1} \sin^2 \Theta + (1-N)^{-1} \cos^2 \Theta]. \quad (5)$$

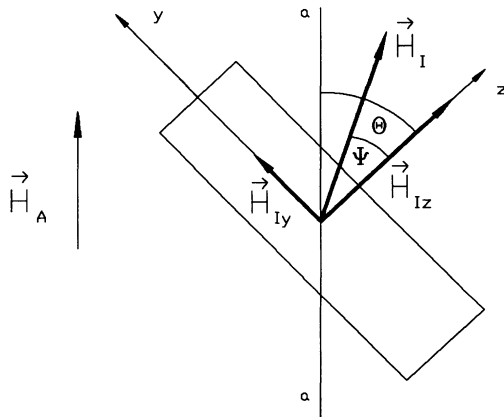


FIG. 1. Internal magnetic field \mathbf{H}_I direction for the “flat” zero-field-cooled sample in applied magnetic field \mathbf{H}_A . a - a line is the magnetometer axis.

The demagnetizing factors M, N calculated from the dimensions of our crystals are given in Table I. Introducing the demagnetizing factors into formula (5), and putting $\chi = -1/4\pi$, we were able to calculate the dependence of M_{ZFC} on the rotation angle for all the crystals without any fitting parameters. The dashed lines in Fig. 2 represent the calculated M_{ZFC} versus the rotation angle Θ . The calculated curves reproduce the experimental data very well.

The striking feature of the results presented in Fig. 2 is

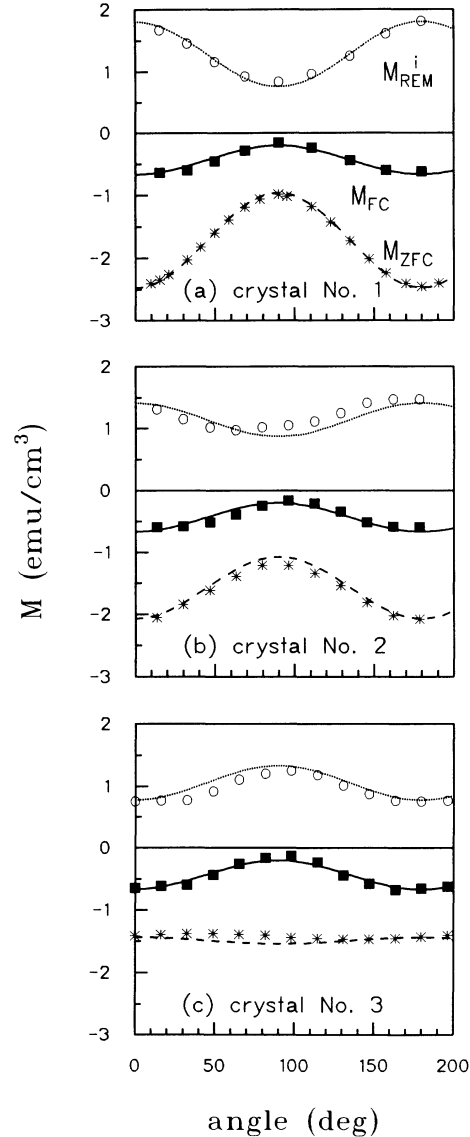


FIG. 2. Angular dependence of zero-field-cooled (M_{ZFC}), field-cooled (M_{FC}), and initial remanent magnetization (M_{REM}^i) for $\text{Pb}_2\text{Sr}_2\text{Y}_{0.3}\text{Ca}_{0.7}\text{Cu}_3\text{O}_8$ single crystals. The horizontal axis is the rotation angle Θ for the ZFC measurements and the cooling angle Φ for the FC and REM measurements. ZFC and FC data were measured at $T = 4.2$ K in $H = 10$ Oe. Dashed lines represent the results of the calculations of M_{ZFC} using Eq. (5). Formula (6) is fitted to the FC magnetization and shown as solid lines. Dotted lines are calculated using the relation $M_{\text{REM}}^i = M_{\text{FC}} - M_{\text{ZFC}}$.

that the dependence of the FC magnetization on the cooling angle is almost identical for all three samples in spite of significant differences on the demagnetizing factor ratios N/M . The results of the cooling-angle dependence of the FC magnetization, $M_{FC}(\Phi)$ for samples 1, 2, 3 are collected in Fig. 3. They can be reasonably approximated by formula

$$M_{FC} \simeq A + B \cos^2 \Phi. \quad (6)$$

The solid line in Fig. 3 is the best fit of formula (6) to the experimental points for all three samples.

The lack of an influence of the demagnetizing effect on the FC magnetization may be explained in the following way. The magnetic susceptibility at the irreversibility line, where the magnetic flux is trapped, is far from the ideal one. Therefore the increase of the internal magnetic field, due to the demagnetization effect, is rather small, according to Eq. (1). Besides, this increase of H_I produces even smaller changes of the magnetization, because the applied magnetic field $H_A = 10$ Oe significantly exceeds H_{c1} at the irreversibility temperature. We conclude, therefore, that the angular dependence of M_{FC} reflects the intrinsic material anisotropy of the crystal. The maximum of M_{FC} observed for the cooling angle $\Phi = 90^\circ$ (i.e., $\mathbf{H} \perp \mathbf{c}$) indicates that the easy axis for flux trapping is parallel to the a - b planes. This observation is in agreement with the anisotropy of the irreversibility line, measured in HTSC.^{10,11} In a given magnetic field, the irreversibility temperature is higher for $\mathbf{H} \perp \mathbf{c}$ than for $\mathbf{H} \parallel \mathbf{c}$. During the cooling process in the magnetic field, the vortices are partially trapped in the a - b planes, when the temperature crosses the upper irreversibility line. Some of the vortices move out from the sample or rotate to align themselves with the a - b planes, as long as the temperature is higher than the temperature of irreversibility along the c axis. As a result the anisotropy of magnetic flux trapping is observed.

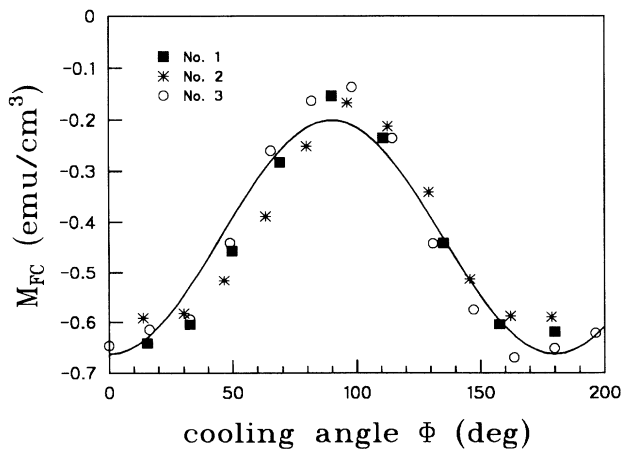


FIG. 3. The field-cooled magnetization for three $\text{Pb}_2\text{Sr}_2\text{Y}_{0.3}\text{Ca}_{0.7}\text{Cu}_3\text{O}_8$ crystals. The samples were cooled down to 4.2 K in magnetic field 10 Oe at the angle Φ between the applied field and c axis of the crystals. Solid line is a fit of formula (6) to the experimental data.

Now, having M_{ZFC} versus rotation angle calculated and M_{FC} versus cooling angle fitted to the experimental points with a formula independent of the shape of the samples, we can calculate M_{REM}^i versus cooling angle exploiting the formula $M_{REM}^i = M_{FC} - M_{ZFC}$. Dotted lines in Fig. 2 represent the remanent magnetization versus cooling angle calculated without any fitting parameters [except for $M_{FC}(\Phi)$, which is taken from experiment] for our crystals. The calculated curves reproduce quite well the values measured for $M_{REM}(\Phi)$ as well as the variation of $M_{REM}(\Phi)$ when the ratio of the demagnetizing factors N/M changes from 3.9 for crystal No. 1 to 0.92 for crystal No. 3. The $M_{REM}(\Phi)$ dependence for crystal No. 3 [Fig. 2(c)] is very slightly affected by the demagnetizing effect (the demagnetizing factor ratio N/M is close to 1) and reflects the intrinsic anisotropy of the magnetic flux trapping. The biggest remanent magnetization was found for the magnetic field parallel to the a - b planes.

We have measured the dependence of all three magnetizations of M_{ZFC} , M_{FC} , and M_{REM} on the rotation angle Θ . The results obtained for two cooling angles $\Phi = 0$ and $\Phi = 60^\circ$ for sample No. 1 are presented in Fig. 4 and show that the sum $M_{FC} = M_{ZFC} + M_{REM}$ is fulfilled very well. Measuring the dependence of M_{ZFC} and M_{REM} on the rotation angle Θ we can easily calculate the angular dependence of M_{FC} . Therefore, we limited our further measurements to the angular dependence of M_{REM} .

The projection of the remanent magnetization on the magnetometer axis (M_{REM}) during the rotation of the sample was measured to determine the direction of the remanent magnetization vector \mathbf{M}_{REM} for various cooling angles. Typical angular dependence of M_{REM} is shown in Fig. 5. The results are fitted by the formula

$$M_{REM}(\Theta) = M_{REM}^{\max} \cos(\Theta - \Theta_M), \quad (7)$$

where Θ_M is the angle at which $M_{REM}(\Theta)$ attains its maximum value during rotation. Θ_M is therefore the angle between the c axis of the crystal and the magnetization vector trapped in the crystal during the cool-

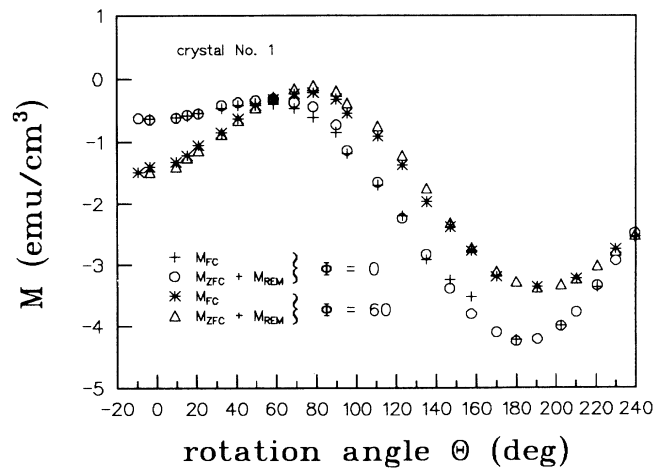


FIG. 4. Angular dependence of the field-cooled magnetization for crystal No. 1 for two cooling angles Φ . For comparison, angular dependence of the sum $M_{ZFC} + M_{REM}$ is shown.

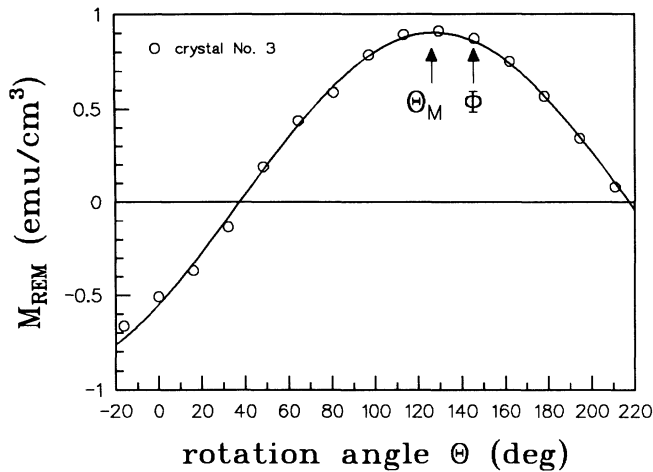


FIG. 5. Angular dependence of the remanent magnetization of the $\text{Pb}_2\text{Sr}_2\text{Y}_{0.3}\text{Ca}_{0.7}\text{Cu}_3\text{O}_8$ single crystal. Φ is a cooling angle between the applied magnetic field and the c axis of the crystal during cooling process. Θ_M is the angle at which the maximum of the magnetization is observed during rotation of the crystal. The solid line is a fit of Eq. (7) to the points.

ing process. Θ_M versus cooling angle for samples No. 1 and No. 3 is presented in Fig. 6. One can observe that the magnetization deviates from the applied field direction toward the c axis for crystal No. 1, but toward the line parallel to the a - b planes for crystal No. 3. We have also calculated Θ_M for isotropic samples with dimensions equal to those of our crystals. In this case, Θ_M is equal to Ψ given by Eq. (4). The calculated angular dependencies of Θ_M are drawn as a solid line for sample No. 1 and a dashed line for sample No. 3. We note only small differences between measured and calculated Θ_M for crystal No. 1, indicating that the direction of the \mathbf{M}_{REM} vector in the crystal is governed mainly by the demagnetizing effect. Substantial deviations of the measured Θ_M from the calculated dependence on the cooling angle Φ for sample No. 3 reflect the material anisotropy of flux trapping. This supports our former conclusion that the a - b plane is the preferred orientation for trapped vortices.

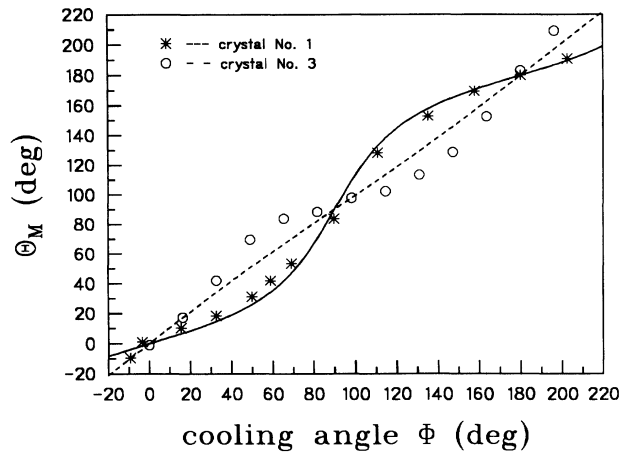


FIG. 6. The angle Θ_M between the applied magnetic field and the direction of the remanent moment as a function of the cooling angle Φ for crystals No. 1 and 3. Solid line and dashed line are the dependencies calculated according to Eq. (4) for isotropic samples with the demagnetizing factors equal to those of samples No. 1 and 3, respectively.

We have found experimentally that the measured FC magnetization of $\text{Pb}_2\text{Sr}_2\text{Y}_{0.3}\text{Ca}_{0.7}\text{Cu}_3\text{O}_8$ crystals is not affected by the demagnetizing effect. Therefore the dependence of the FC magnetization on the cooling angle reflects the pinning anisotropy only. The preferred direction for flux trapping is parallel to the a - b planes. We have shown, that the angular dependencies of the ZFC and REM magnetizations can be calculated (in good agreement with the experimental data) from the dimensions of the crystals, taking into account the demagnetizing effect and the magnetization versus cooling angle dependence. The angular dependence of the REM magnetization is affected by the material anisotropy and the demagnetizing effect. The results of the measurements of the REM magnetization versus the rotation angle on crystal No. 3 support the conclusion, that the easy axis for flux trapping is parallel to the a - b planes.

This work was funded in part by KBN under Contract No. 711/2/91.

¹J. R. Clem, *Physica C* **162-164**, 1137 (1989).

²V. G. Kogan, *Physica C* **162-164**, 1689 (1989).

³E. H. Brandt, *Physica B* **169**, 91 (1991).

⁴M. Tachiki and S. Takahashi, *Solid State Commun.* **70**, 291 (1989).

⁵I. Felner, U. Yaron, Y. Yeshurun, G. V. Chandrashekar, and F. Holtzberg, *Phys. Rev. B* **40**, 5239 (1989).

⁶M. Tuominen, A. M. Goldman, Y. C. Chang, and P. Z. Jiang, *Phys. Rev. B* **42**, 8740 (1990).

⁷Comment on Ref. 1 in S. Kolesnik, T. Skośkiewicz, and J. Igalsón, *Phys. Rev. B* **43**, 13 679 (1991) and Felner's *et al.*

reply, *Phys. Rev. B* **43**, 13 681 (1991).

⁸Z. Korczak, W. Korczak, S. Kolesnik, T. Skośkiewicz, and J. Igalsón, *Supercond. Sci. Technol.* **3**, 370 (1990).

⁹Definition of demagnetizing factors follows by M. W. Denhoff and Suso Cygax, *Phys. Rev. B* **25**, 4479 (1982).

¹⁰B. D. Biggs, M. N. Kunchur, J. J. Lin, S. J. Poon, T. R. Askew, R. B. Flippen, M. A. Subramanian, J. Gopalakrishnan, and A. W. Sleight, *Phys. Rev. B* **39**, 7309 (1989).

¹¹H. W. Weber and G. W. Crabtree, in *Studies of High Temperature Superconductors*, edited by A. V. Narlikar (Nova Science, New York, to be published).